

# Reflection of Plane Wave at Traction-Free Surface of a Pre-Stressed Functionally Graded Piezoelectric Material (FGPM) Half-Space

P.K. Saroj<sup>\*</sup>, S.A. Sahu

*Department of Applied Mathematics, Indian Institute of Technology (ISM), Dhanbad-826004, India*

Received 23 March 2017; accepted 19 May 2017

## ABSTRACT

This paper is devoted to study a problem of plane waves reflection at a traction-free surface of a pre-stressed functionally graded piezoelectric material (FGPM). The effects of initial stress and material gradient on the reflection of plane waves are studied in this paper. Secular equation has been derived analytically for the pre-stressed FGPM half-space and used to show the existence of two coupled waves namely  $qP$  and  $qSV$ . Continuity condition of stress, electrical potential and electrical displacement at traction free surface is used to obtain the reflection coefficient of  $qP$  and  $qSV$  waves. Results of the problem are shown graphically and effects of initial stress and material gradient are discussed for a particular case of Lithium niobate material.

© 2017 IAU, Arak Branch. All rights reserved.

**Keywords :** Piezoelectricity; Reflection; Traction-free surface; Reflection coefficient.

## 1 INTRODUCTION

THE study of reflection and refraction phenomenon in piezoelectric materials has gained considerable attention due to their important role in hydrophone technology, aerospace engineering, civil engineering and in general ultrasonic transducer application. Reflection and transmission of acoustic energy at boundary surface plays an important role in the area like signal processing, transduction and frequency control. Piezoelectric solids are inherently anisotropic and layered arrangement of piezoelectric material has been used for different purposes. The layered arrangement is easy to realize experimentally and modification can be made easily by different choice of material. In recent years use of piezoelectric materials in device applications has made this area of a great importance. It has attracted the attention of researchers to study reflection and refraction phenomenon at the interface between a piezoelectric crystal and viscous conductive liquid for bulk wave liquid sensors [1], piezoelectric ceramics and water [2]. Chattopadhyay and Saha [3] studied the phenomenon of reflection and refraction of  $P$  waves at the interface of monoclinic media and prove the predominant effect of material constants. Kaur and Tomar [4] discussed the effect of corrugation and elastic properties on reflection and transmission coefficients of SH-waves in monoclinic half spaces. Kyame [5] has studied the propagation of plane waves in piezoelectric medium. Yang [6] has presented a review on special topics in piezoelectricity. A brief study has been done by Fang et al. [7] on surface acoustic waves (SAW) propagating over a piezoelectric half-space rotating at a constant angular rate. Wang [8] studied the SH- wave propagation in a semi-infinite solid medium surface bonded by a layer of piezoelectric material abutting the vacuum. Yang and Zhou [9] have discussed various problems of

<sup>\*</sup>Corresponding author. Tel.: +91 9534053582.

E-mail address: pksaroj.ism@gmail.com (P.K. Saroj).

surface wave propagation in piezoelectric coupled media. Pang et al. [10] analyze the reflection and refraction of a plane wave incidence obliquely at the interface between piezoelectric and piezomagnetic media. Sharma et al. [11] have presented a study of propagation and reflection characteristics of waves from the stress free, thermally insulated/isothermal boundary of a piezothermoelastic half space. Chattopadhyay et al. [12] studied the reflection and transmission of shear waves in monoclinic media. Propagation of Rayleigh surface waves in homogeneous, transversely isotropic, piezothermoelastic semi-space has been discussed by Sharma and Walia [13]. Due to non uniform material properties, coefficient of thermal expansion, chemical shrinkage during the processing and cool down to operating and room temperature, the presence of initial stress is unavoidable. Piezoelectric materials are pre-stressed during manufacturing process to avoid brittle fracture. Many authors have studied the effect of initial stress on wave propagation in piezoelectric layered structure. Abd-alla and Alsheikh [14] studied a problem of reflection and refraction of quasi-longitudinal waves under initial stresses at an interface of two anisotropic piezoelectric media with different properties. Singh [15] studied the reflection of plane waves at a traction-free surface of a pre-stressed piezoelectric half-space. Guo and Wei[16] studied the effect of initial stress on the reflection and transmission waves at the interface between two piezoelectric half-spaces. Up to now, no attempt has been made to investigate the wave reflection and refraction in pre-stressed functionally graded piezoelectric material (FGPM).

The present paper studies the reflection phenomenon of plane waves at the traction free surface of a functionally graded piezoelectric medium. Moreover, instead of only consideration of the normal initial stress in most literature, three types of initial stress including normal and shear initial stress are considered. As a salient outcome of the current study, the effect of initial stress and material gradient on the reflection coefficient has been obtained and presented by the means of the graph. Furthermore, graphical representation has been made to compare the reflection coefficient and speed of plane waves in FGPM, pre-stressed FGPM and piezoelectric medium.

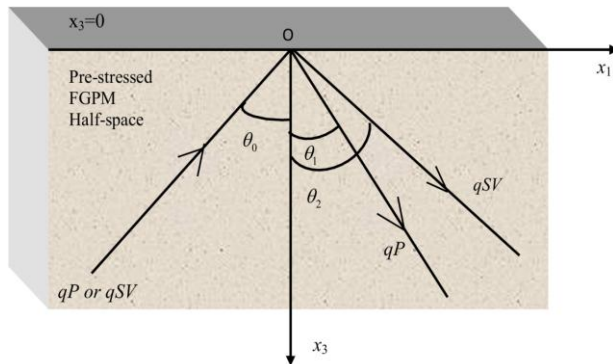


**Fig.1**  
Geometry of the problem.

## 2 STATEMENT OF THE PROBLEM

Here we consider the reflection of plane waves ( $qP$  or  $qSV$ ) at a traction-free and electrically shorted/charge free surface of a pre-stressed transversely isotropic functionally graded piezoelectric material half-space. We have considered the rectangular coordinate system  $(x_1, x_2, x_3)$  with the  $x_3$ -axis directed vertically downwards. The plane  $x_2 = 0$  is assumed to be the plane of incidence.

For the piezoelectric layer with initial stress, the equilibrium equations of elasticity without body forces and the Gauss' law of electrostatics without free charge are given as follows (Wang and Shang [17])

$$\sigma_{ij,j} + (u_{i,k} \sigma_{kj}^0)_{,j} = \rho \ddot{u}_i, \quad D_{i,i} = 0 \quad (1)$$

where  $i, j, k = 1, 2, 3$ ,  $\rho$  is the mass density,  $u_i$  and  $D_i$  denote the mechanical and electric displacements in the  $i$ th direction respectively,  $\sigma_{ij}$  is the stress tensor,  $\sigma_{kj}^0$  is the initial stress tensor. The dots denote time differentiation, the comma denotes space-coordinate differentiation.

The well-known piezoelectric constitutive equations are

$$\sigma_{ij} = c_{ijkl} S_{kl} - e_{kij} E_k, \quad D_j = e_{jkl} S_{kl} + \epsilon_{jk} E_k \tag{2}$$

where  $\sigma_{ij}$  and  $S_{kl}$  are the stress and strain tensor.  $D_j$  and  $E_k$  are the electrical displacement and field intensity,  $c_{ijkl}, e_{kij}, \epsilon_{jk}$  are the elastic, piezoelectric and dielectric coefficients respectively. For transversely isotropic material Eq. (2) can be written as:

$$\begin{Bmatrix} \sigma_{x_1x_1} \\ \sigma_{x_2x_2} \\ \sigma_{x_3x_3} \\ \sigma_{x_2x_3} \\ \sigma_{x_3x_1} \\ \sigma_{x_1x_2} \end{Bmatrix} = \begin{bmatrix} c_{11} & c_{12} & c_{13} & 0 & 0 & 0 \\ c_{12} & c_{11} & c_{13} & 0 & 0 & 0 \\ c_{13} & c_{13} & c_{13} & 0 & 0 & 0 \\ 0 & 0 & 0 & c_{44} & 0 & 0 \\ 0 & 0 & 0 & 0 & c_{44} & 0 \\ 0 & 0 & 0 & 0 & 0 & 0.5(c_{11} - c_{12}) \end{bmatrix} \cdot \begin{Bmatrix} S_{x_1x_1} \\ S_{x_2x_2} \\ S_{x_3x_3} \\ S_{x_2x_3} \\ S_{x_3x_1} \\ S_{x_1x_2} \end{Bmatrix} - \begin{bmatrix} 0 & 0 & e_{31} \\ 0 & 0 & e_{31} \\ 0 & 0 & e_{33} \\ 0 & e_{15} & 0 \\ e_{15} & 0 & 0 \\ 0 & 0 & 0 \end{bmatrix} \cdot \begin{Bmatrix} E_{x_1} \\ E_{x_2} \\ E_{x_3} \end{Bmatrix} \tag{3a}$$

$$\begin{Bmatrix} D_{x_1} \\ D_{x_2} \\ D_{x_3} \end{Bmatrix} = \begin{bmatrix} 0 & 0 & 0 & 0 & e_{15} & 0 \\ 0 & 0 & 0 & e_{15} & 0 & 0 \\ e_{31} & e_{31} & e_{33} & 0 & 0 & 0 \end{bmatrix} \cdot \begin{Bmatrix} S_{x_1x_1} \\ S_{x_2x_2} \\ S_{x_3x_3} \\ S_{x_2x_3} \\ S_{x_3x_1} \\ S_{x_1x_2} \end{Bmatrix} + \begin{bmatrix} \epsilon_{11} & 0 & 0 \\ 0 & \epsilon_{111} & 0 \\ 0 & 0 & \epsilon_{33} \end{bmatrix} \cdot \begin{Bmatrix} E_{x_1} \\ E_{x_2} \\ E_{x_3} \end{Bmatrix} \tag{3b}$$

In the plane strain case, the displacement and electric potential are only the function of  $x_1$  and  $x_3$ . We have the following equation of motion for pre-stressed transversely isotropic functionally graded piezoelectric material obtained after recalling Eqs. (1) - (2) and Eq. (3a)-(3b).

$$\begin{aligned} c_{11}\sigma_{11,1} + \sigma_{13,3} + (u_{1,11}\delta_{11}^0 + 2u_{1,31}\delta_{31}^0 + u_{1,33}\delta_{33}^0) + (u_{1,1}\delta_{11,1}^0 + u_{1,3}\delta_{31,1}^0 + u_{1,1}\delta_{31,3}^0 + u_{1,3}\delta_{33}^0) &= \rho\ddot{u}_1, \\ \sigma_{13,1} + \sigma_{33,3} + (u_{3,11}\delta_{11}^0 + 2u_{3,31}\delta_{31}^0 + u_{3,33}\delta_{33}^0) + (u_{3,1}\delta_{11,1}^0 + u_{3,3}\delta_{31,1}^0 + u_{3,1}\delta_{31,3}^0 + u_{3,3}\delta_{33}^0) &= \rho\ddot{u}_3, \\ D_{1,1} + D_{3,3} &= 0. \end{aligned} \tag{4}$$

The initial stress and elastic constants of FGPM half-space have an exponential variation of the form

$$c_{ij}(x_3) = c_{ij}^0 e^{\beta x_3}, e_{ij}(x_3) = e_{ij}^0 e^{\beta x_3}, \epsilon_{ij}(x_3) = \epsilon_{ij}^0 e^{\beta x_3}, \rho(x_3) = \rho^0 e^{\beta x_3}, \sigma_{ij}^0(x_3) = \sigma_{ij}^0 e^{\beta x_3} \tag{5}$$

where  $\beta > 0$  is the gradient factor and  $c_{ij}^0, e_{ij}^0, \epsilon_{ij}^0, \rho^0, \sigma_{ij}^0$  are the values of  $c_{ij}, e_{ij}, \epsilon_{ij}, \rho, \sigma_{ij}$  on the surface.

So the equation of motion (4), with the help of Eq. (5) reduces to

$$c_1^* u_{1,11} + c_2^* u_{1,33} + c_5^* u_{3,13} + 2u_{1,31}\sigma_{31}^0 + (e_{15}^0 + e_{13}^0)\phi_{,13} + \beta c_1^* u_{1,1} + \beta u_{1,3}\sigma_{31}^0 + \beta c_{13}^0 u_{3,3} + \beta e_{13}^0 \phi_{,3} = \rho^0 \ddot{u}_1, \tag{6}$$

$$c_4^* u_{3,11} + c_3^* u_{3,33} + c_5^* u_{1,13} + 2u_{3,31}\sigma_{31}^0 + e_{15}^0 \phi_{,11} + e_{33}^0 \phi_{,33} + \beta c_4^* u_{3,1} + \beta c_{44}^0 u_{1,3} + \beta \sigma_{31}^0 u_{3,3} + \beta e_{15}^0 \phi_{,1} = \rho^0 \ddot{u}_3, \tag{7}$$

$$(e_{15}^0 + e_{13}^0)u_{1,13} + e_{15}^0 u_{3,11} + e_{33}^0 u_{3,33} - \epsilon_{11}^0 \phi_{,11} - \epsilon_{33}^0 \phi_{,33} + \beta (e_{15}^0 u_{1,3} + e_{15}^0 u_{3,1} - \epsilon_{11}^0 \phi_{,1}) = 0. \tag{8}$$

where

$$c_1^* = c_{11}^0 + \sigma_{11}^0, c_2^* = c_{44}^0 + \sigma_{33}^0, c_3^* = c_{33}^0 + \sigma_{33}^0, c_4^* = c_{44}^0 + \sigma_{11}^0, c_5^* = c_{44}^0 + c_{13}^0.$$

Consider a plane wave solution of Eqs. (6)-(8) of the form

$$\begin{pmatrix} u_1 \\ u_3 \\ \phi \end{pmatrix} = \begin{pmatrix} Ad_1 \\ Ad_3 \\ B \end{pmatrix} e^{ik(x_1 p_1 + x_3 p_3 - ct)} \quad (9)$$

where  $(p_1, p_3)$  are the unit propagation vectors,  $(d_1, d_3)$  are the displacement vectors,  $A, B$  are the wave amplitude and  $c$  is the phase speed respectively.

Inserting the representation (9) into Eqs. (6)-(8), we obtained the Christoffel equation of the form

$$\begin{bmatrix} K_{11} & K_{12} & K_{13} \\ K_{21} & K_{22} & K_{23} \\ K_{31} & K_{32} & K_{33} \end{bmatrix} \begin{Bmatrix} Ad_1 \\ Ad_3 \\ B \end{Bmatrix} = 0 \quad (10)$$

The explicit expressions of elements in the matrix are

$$\begin{aligned} K_{11} &= D_1 + ic_1 - m, K_{12} = L_1 + ic_2, K_{13} = L_2 + ic_3, \\ K_{21} &= L_1 + id_1, K_{22} = D_2 + id_2 - m, K_{23} = D_4 + id_3, \\ K_{31} &= L_2 + ie_1, K_{32} = D_4 + ie_2, K_{33} = -D_3 + ie_3, \end{aligned} \quad (11)$$

where  $m = \rho^0 c^2$  and definitions of  $D_i$ 's,  $L_i$ 's,  $d_i$ 's,  $c_i$ 's,  $e_i$ 's are given as:

$$\begin{aligned} D_1 &= c_1^* p_1^2 + c_2^* p_3^2 + 2\sigma_{13}^0 p_1 p_3, \quad D_2 = c_4^* p_1^2 + c_3^* p_3^2 + 2\sigma_{13}^0 p_1 p_3, \quad D_3 = \varepsilon_{11}^0 p_1^2 + \varepsilon_{33}^0 p_3^2, \quad D_4 = e_{13}^0 p_1^2 + e_{33}^0 p_3^2, \\ L_1 &= c_5^* p_1 p_3, \quad L_2 = (e_{15}^0 + e_{31}^0) p_1 p_3, \\ c_1 &= \frac{\beta(c_1^* p_1 + \sigma_{13}^0 p_3)}{k}, \quad c_2 = \frac{\beta(c_3^* p_3)}{k}, \quad c_3 = \frac{\beta(e_{13}^0 p_3)}{k}, \\ d_1 &= \frac{\beta(c_{44}^0 p_3)}{k}, \quad d_2 = \frac{\beta(c_4^* p_1 + \sigma_{13}^0 p_3)}{k}, \quad d_3 = \frac{\beta(e_{15}^0 p_1)}{k}, \\ e_1 &= \frac{\beta(e_{15}^0 p_3)}{k}, \quad e_2 = \frac{\beta(e_{15}^0 p_1)}{k}, \quad e_3 = \frac{\beta(\varepsilon_{11}^0 p_1)}{k}. \end{aligned}$$

The characteristic equation is derived with the help of Eqs. (10). Setting the characteristic determinant of the Christoffel equation equal to zero we have

$$m^2 (D_3^2 + e_3^2) - m (B_1 + iB_2)(D_3 + ie_3) - (A_1 + iA_2)(D_3 + ie_3) = 0. \quad (12)$$

where the definitions of  $A_1, A_2$  and  $B_1, B_2$  are given as:

$$\begin{aligned} A_1 &= c_1 d_2 D_3 + c_1 d_3 D_4 + e_2 d_3 D_1 + c_1 e_2 D_4 - d_2 e_3 D_1 - c_1 e_3 D_2 - d_1 c_3 D_4 + d_2 e_1 L_2 + e_1 c_3 D_2 - d_1 e_2 L_2 + d_2 c_3 L_2 - \\ &\quad e_2 c_3 L_2 - c_2 d_1 D_3 - c_2 e_1 D_4 + c_2 e_3 L_1 - c_2 d_3 L_2 - d_3 e_1 L_1 + d_1 e_3 L_1 - D_1 D_2 D_3 - D_1 D_4^2 + 2L_1 L_2 D_4 - D_2 L_2^2 + D_3 L_1^2, \\ A_2 &= -d_2 D_1 D_3 - c_1 D_2 D_3 - d_3 D_1 D_4 - c_1 D_4^2 - c_1 c_2 d_3 - e_2 D_1 D_4 + c_1 d_2 e_3 + e_3 D_1 D_2 + d_1 D_4 L_2 - e_1 d_2 c_3 - e_1 D_2 L_2 + d_1 e_2 c_3 \\ &\quad + c_3 D_4 L_1 - d_2 L_2^2 - c_3 D_2 L_2 + e_2 L_2^2 + e_1 c_2 d_3 - d_1 c_2 e_3 + c_2 D_3 L_1 + c_2 D_4 L_2 + d_1 L_1 D_3 + e_1 D_4 L_1 - e_3 L_1^2 + d_3 L_1 L_2, \end{aligned}$$

$$B_1 = D_1D_3 + D_2D_3 + D_4^2 + L_2^2 - d_3e_2 + e_3c_1 + d_2e_3 - e_1c_3,$$

$$B_2 = c_1D_3 + d_2D_3 + d_3D_4 + e_2D_4 - e_3D_1 - e_3D_2.$$

The boundary conditions at traction free and electrically shorted/charge free surface can be listed as:

$$\sigma_{33} + u_{3,1}\sigma_{31}^0 + u_{3,3}\sigma_{33}^0 = 0, \tag{13}$$

$$\sigma_{31} + u_{1,1}\sigma_{31}^0 + u_{1,3}\sigma_{33}^0 = 0, \tag{14}$$

$$\phi = 0, \text{ (electrically shorted surface)} \tag{15}$$

$$D_3 = 0. \text{ (charge free case)} \tag{16}$$

An incident ( $qP$  or  $qSV$ ) waves, making an angle  $\theta_0$  with normal to the interface  $x_3 = 0$  is considered. Upon reflection at the interface, an incident waves (identified by  $n = 0$ ) gives rise two reflected wave (identified by subscript  $n = 1,3$ ). The displacements and the scalar electric potential of the incident and reflected wave are represented by

$$u_j^n = A_n d_j^{(n)} \exp\left(ik_n (x_1 p_1^n + x_3 p_3^n - c_n t)\right), \quad j = 1,3. \tag{17}$$

$$\phi^n = F_n A_n \exp\left(ik_n (x_1 p_1^n + x_3 p_3^n - c_n t)\right). \tag{18}$$

where  $d^{(n)}$  is the unit displacement vector,  $A_n, F_n$  is the amplitude of the wave travelling with speed  $c_n, k_n$  is the wave number specified with unit direction  $p^{(n)}$ . For the electrically shorted surface, from Eq. (15)

$$F_n = 0, \tag{19}$$

and for charge-free surface we have

$$F_n = \frac{e_{31}^0 p_1^{(n)} + e_{33}^0 p_3^{(n)}}{\epsilon_{33}^0 p_3^{(n)}}. \tag{20}$$

with the help of Eqs. (13) - (18), we have in general

$$G_n A_n e^{ik_n (x_1 p_1^{(n)} + x_3 p_3^{(n)} - c_n t)} = 0, \tag{21}$$

$$H_n A_n e^{ik_n (x_1 p_1^{(n)} + x_3 p_3^{(n)} - c_n t)} = 0. \tag{22}$$

From Eqs.(20)-(22), we have for the electrically shorted case

$$G_n = k_n \left[ c_{13}^0 p_1^{(n)} d_1^{(n)} + \left( c_3^* p_3^{(n)} + \sigma_{13}^0 p_1^{(n)} \right) d_3^{(n)} \right], \tag{23}$$

$$H_n = k_n \left[ c_{44}^0 p_1^{(n)} d_3^{(n)} + \left( c_2^* p_3^{(n)} + \sigma_{13}^0 p_1^{(n)} \right) d_1^{(n)} \right], \tag{24}$$

and for the charge free case

$$G_n = k_n \left[ \left( c_{13}^0 + \frac{e_{13}^0}{\varepsilon_{33}^0} \right) p_1^{(n)} d_1^{(n)} + \left( \left( c_3^* + \frac{e_{33}^0}{\varepsilon_{33}^0} \right) p_3^{(n)} + \sigma_{13}^0 p_1^{(n)} \right) d_3^{(n)} \right], \quad (25)$$

$$H_n = k_n \left[ c_{44}^0 p_1^{(n)} d_3^{(n)} + \left( c_2^* p_3^{(n)} + \sigma_{13}^0 p_1^{(n)} \right) d_1^{(n)} + e_{15}^0 \left( \frac{e_{13}^0}{\varepsilon_{33}^0} p_1^{(n)} d_1^{(n)} + \frac{e_{33}^0}{\varepsilon_{33}^0} p_3^{(n)} d_1^{(n)} \right) \frac{p_1^{(n)}}{p_3^{(n)}} \right]. \quad (26)$$

The above equations are valid for all values of  $x_1$  and  $t$ , so that we have

$$k_0 p_1^{(0)} = k_1 p_1^{(1)} = k_2 p_1^{(2)} = k, \quad k_0 c_0 = k_1 c_1 = k_2 c_2 = \omega, \quad (27)$$

where  $k$  and  $\omega$  are apparent wave number and circular frequency, respectively. The amplitude ratios are then obtained from Eqs. (23)-(24) and (25)-(26) as:

$$R_1 \equiv \frac{A_1}{A_0} = \frac{G_2 H_0 - H_2 G_0}{G_1 H_2 - H_1 G_2}, \quad R_2 \equiv \frac{A_2}{A_0} = \frac{H_1 G_0 - G_1 H_0}{G_1 H_2 - H_1 G_2}. \quad (28)$$

### 3 NUMERICAL RESULTS AND DISCUSSION

In order to illustrate theoretical results in the proceeding sections, we now present some numerical results. The material constant of Lithium niobate crystal has been considered for this purpose. This material finds application in optical waveguides, piezoelectric sensors, and optical modulators. Two cases, incident  $qP$  waves and incident  $qSV$  waves are considered in the numerical example for charge free and electrically shorted case. The physical parameters of Lithium niobate material are [18]

$$c_{11}^0 = 2.03 \times 10^{11} \text{ N / m}^2, c_{33}^0 = 2.424 \times 10^{11} \text{ N / m}^2, c_{44}^0 = 0.595 \times 10^{11} \text{ N / m}^2, c_{13}^0 = 0.752 \times 10^{11} \text{ N / m}^2, \\ e_{13}^0 = 0.23 \text{ C / m}^2, e_{33}^0 = 1.33 \text{ C / m}^2, e_{15}^0 = 3.7 \text{ C / m}^2, \varepsilon_{11}^0 = 85.2, \varepsilon_{33}^0 = 28.7, \rho = 4.647 \times 10^3 \text{ kg / m}^3.$$

The following non dimensional parameters have been also used for calculation

$$\sigma_{11}^{0*} = 0.41, \sigma_{13}^{0*} = -0.25, \sigma_{33}^{0*} = 0.41.$$

#### 3.1 INCIDENT $qP$ WAVES

Figs. 2 and 3 show the variation of speeds of reflected  $qP$  and  $qSV$  waves with the angle of incidence  $\theta_0$ . The curves show the variation of speed against the angle of incidence in pre-stressed FGPM, FGPM and piezoelectric material for charge free surface. The curves clearly show that pre-stressed FGPM has higher speed (for  $qP$  and  $qSV$  wave). The speed of  $qP$  waves decreases in a piezoelectric medium as the angle of incidence  $\theta_0$  changes from normal incidence to grazing incidence. The speed of  $qSV$  waves decreases sharply for  $\theta_0 > 40$ . Variation of reflection coefficient of  $qP$  and  $qSV$  waves in the case of incident  $qP$  waves are shown in Figs. 4 and 5. It is clear from the curves that the reflection coefficient of  $qP$  waves in functionally graded piezoelectric material is higher as compared to FGPM and piezoelectric medium. The maximum value of reflection coefficient is at  $80^\circ$  in pre-stressed FGPM, FGPM and  $60^\circ$  in piezoelectric medium. From Fig. 5 we can say that FGPM medium has a higher

reflection coefficient of  $qSV$  waves. It is also found that reflection coefficient of  $qSV$  waves decrease sharply after  $20^\circ$  angle of incidence. The effects of material gradient  $\beta$  are shown in Figs. 6. It is found that reflection coefficient of  $qP$  waves increases with the increase of material gradient for  $\theta_0 < 40$  and decreases with the increase of material gradient for angle of incidence  $\theta_0 > 40$ . Fig. 7 shows the effect of initial stress  $\sigma_{xx}^0$  on the reflection coefficient of  $qP$  waves. The reflection coefficient of  $qP$  waves decreases for  $\theta_0 < 35$  and increases for  $\theta_0 > 35$  as the value of initial stress  $\sigma_{xx}^0$  increases. The effects of initial stress  $\sigma_{xz}^0$  are shown in Figs. 8. It is found that reflection coefficient of  $qP$  waves is increasing as the value of initial stress increases. The effects of initial stress  $\sigma_{zz}^0$  are shown in Figs. 9. It is found that the reflection coefficient of  $qP$  waves decreases with the increase of initial stress  $\sigma_{zz}^0$ . Figs. 10-13 show the effects of material gradient, initial stresses ( $\sigma_{xx}^0, \sigma_{xz}^0, \sigma_{zz}^0$ ) for electrically shorted case of incident  $qP$  waves. The effects of these parameters on reflection coefficient are same as in the case of charge free case of incidence  $qP$  waves.

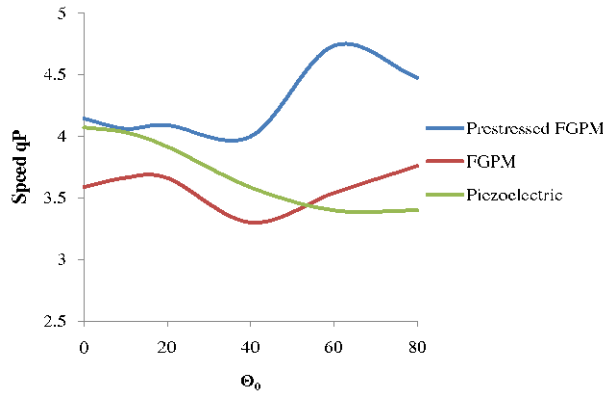


**Fig.2**  
Variations of speeds of reflected  $qP$  waves with angle of incidence  $\theta_0$ .

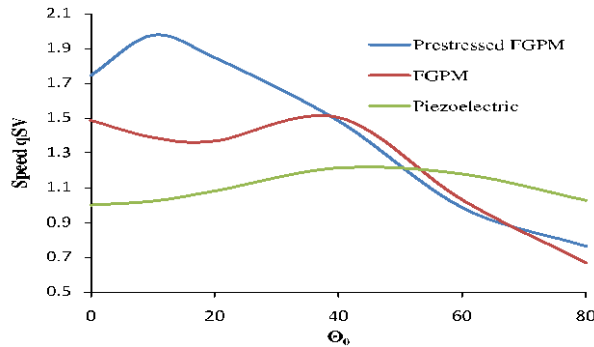


**Fig.3**  
Variations of speeds of reflected  $qSV$  waves with angle of incidence  $\theta_0$ .

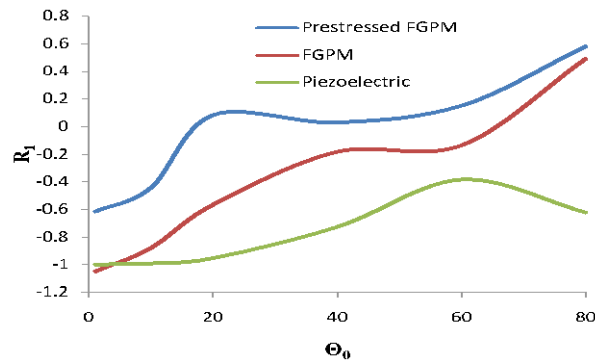


**Fig.4**  
Amplitude ratios of reflected  $qP$  waves in charge free case.

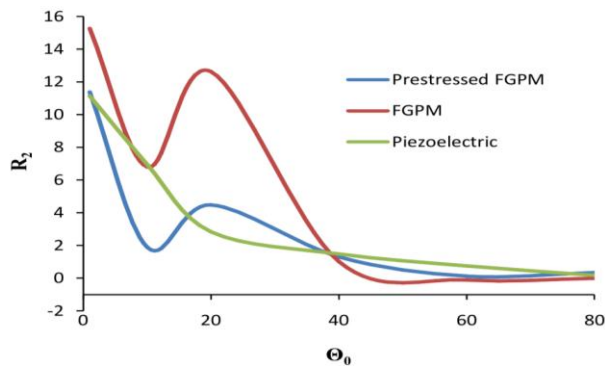


**Fig.5**  
Amplitude ratios of reflected  $qSV$  waves in charge free case.

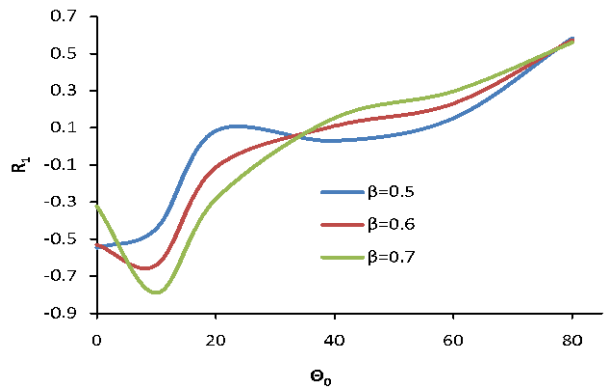


**Fig.6**  
Effect of material gradient on reflection coefficient of reflected  $qP$  waves (Charge free case).

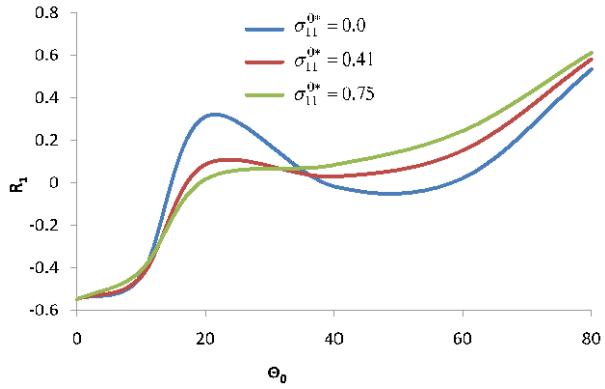


**Fig.7**  
Effect if initial stress  $\sigma_{11}^{0*}$  on the reflection coefficient in the case of incident  $qP$  waves (Charge free case).

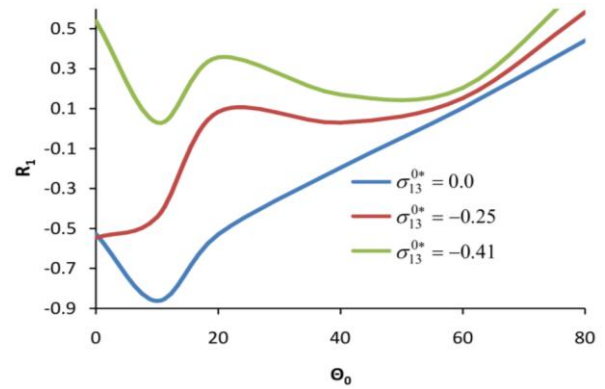


**Fig.8**  
Effect if initial stress  $\sigma_{13}^{0*}$  on the reflection coefficient of  $qP$  wave in the case of incident  $qP$  waves (Charge free case).

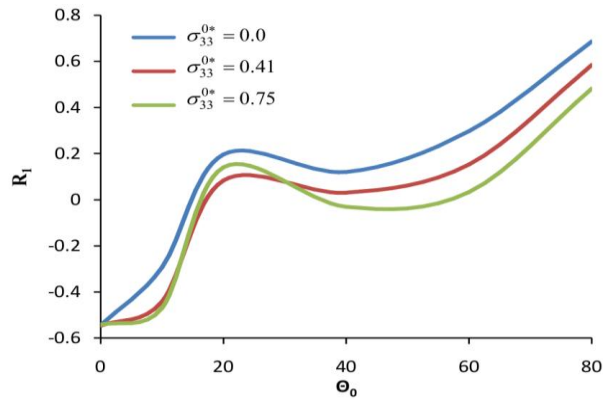


**Fig.9** Effect if initial stress  $\sigma_{33}^{0*}$  on the reflection coefficient of  $qP$  wave in the case of incident  $qP$  waves (Charge free case).

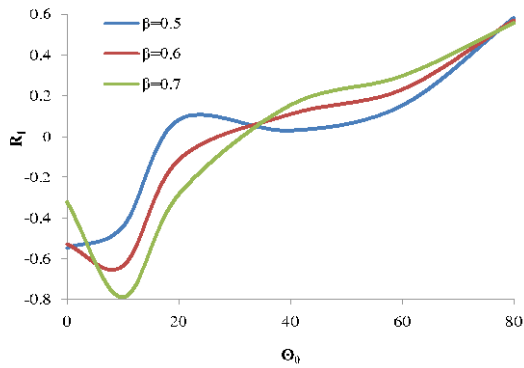


**Fig.10** Effect of material gradient on reflection coefficient of reflected  $qP$  waves (Electrically shorted case).

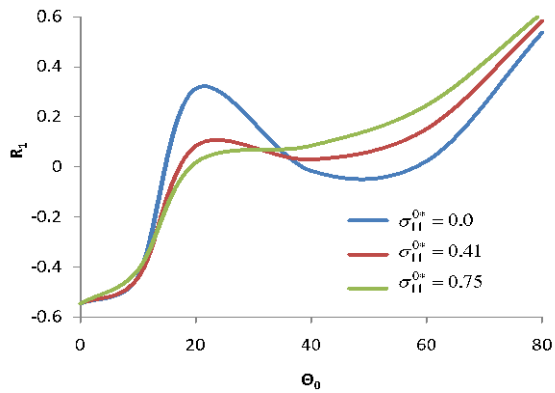


**Fig.11** Effect if initial stress  $\sigma_{11}^{0*}$  on the reflection coefficient of  $qP$  wave in the case of incident  $qP$  waves (Electrically shorted case).

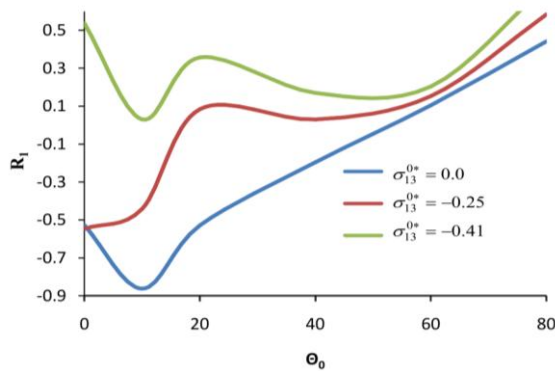


**Fig.12** Effect if initial stress  $\sigma_{13}^{0*}$  on the reflection coefficient of  $qP$  waves in the case of incident  $qP$  waves (Electrically shorted case).

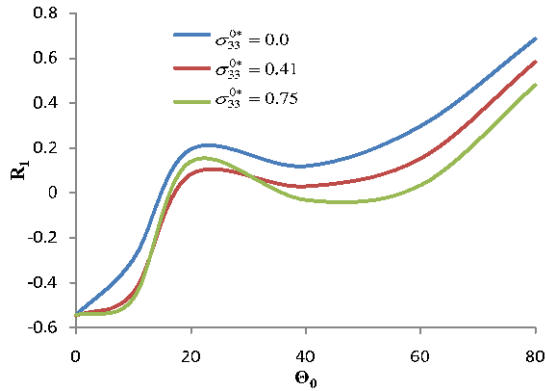


**Fig.13**  
Effect if initial stress  $\sigma_{33}^{0*}$  on the reflection coefficient of  $qP$  waves in the case of incident  $qP$  waves (Electrically shorted case).

3.2 INCIDENT  $qSV$  WAVE

Fig. 14 shows the effect of material gradient on reflection coefficient of reflected  $qSV$  waves in the case of incident  $qSV$  waves. The curves clearly indicate that for  $\theta_0 < 22$  there is no effect of material gradient on reflection coefficient of  $qSV$  waves. It is also observed that for  $22 < \theta_0 < 50$  reflection coefficient of  $qSV$  waves decreasing and that for  $\theta_0 > 50$  it is vice versa. Fig. 15 shows the effect of initial stress  $\sigma_{xx}^0$  on the reflection coefficient of  $qSV$  for incident  $qSV$  waves. It can be observed that for  $\theta_0 < 20$  there is no effect of initial stress on reflection coefficient. It is also observed that for  $20 < \theta_0 < 44$  reflection coefficient of wave decreasing and that for  $\theta_0 > 44$  is increasing. Figs. 16-17 show the effect of initial stress  $\sigma_{xz}^0$  and  $\sigma_{zz}^0$ . The curves clearly show that the amplitude ratio of  $qSV$  first remains constant then increases and again decreases as the angle of incidence of  $qSV$  waves increases.

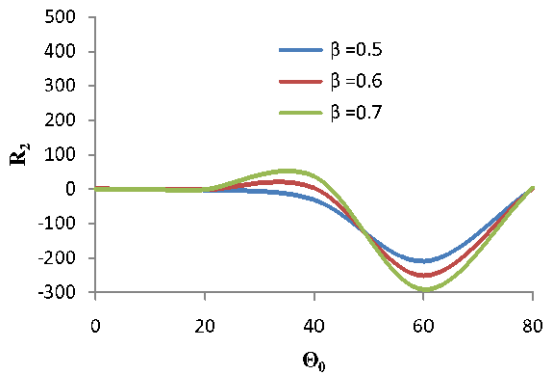


**Fig.14**  
Effect of material gradient on reflection coefficient of  $qSV$  waves in the case of incident  $qSV$  waves (Charge Free case).

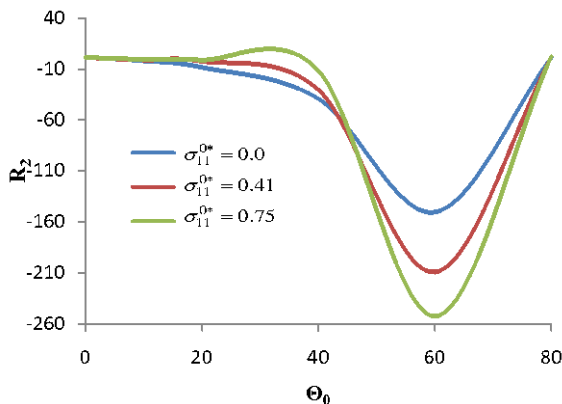


**Fig.15**  
Effect if initial stress  $\sigma_{11}^{0*}$  on the reflection coefficient of  $qSV$  waves in the case of incident  $qSV$  waves (Charge Free case).

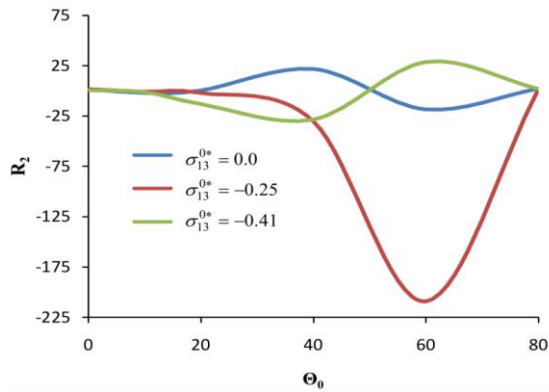


**Fig.16**  
Effect if initial stress  $\sigma_{13}^{0*}$  on the reflection coefficient of  $qSV$  in the case of incident wave (Charge Free case).

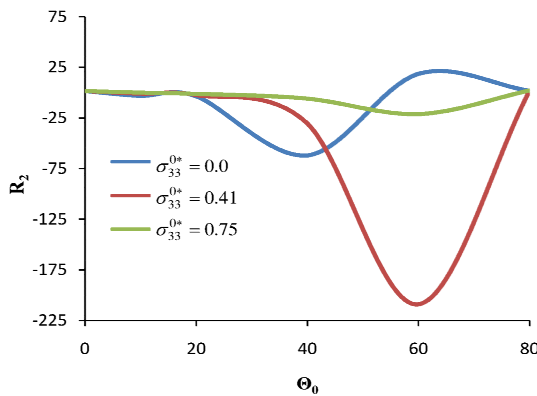


**Fig.17**  
Effect if initial stress  $\sigma_{33}^{0*}$  on the reflection coefficient of  $qSV$  waves in the case of incident  $qSV$  waves (Charge free case).

In order to show the effects of material gradient and initial stress, reflection coefficients ( $R_1$  and  $R_2$ ) are computed for different incident angle  $\theta_0$  with the normal to stress free and electrically shorted/charge free surface. Three kind of initial stresses namely,  $\sigma_{xx}^0, \sigma_{xz}^0$  and  $\sigma_{zz}^0$  are considered for incident  $qP$  and  $qSV$  waves respectively.

#### 4 CONCLUSIONS

Tow dimensional secular equations in transversely isotropic piezoelectric half-space are derived from the general dynamic equation with initial stress. Continuity conditions of stress, electrical displacement and electrical potential at a traction-free surface are used to show the existence of two coupled wave namely  $qP$  and  $qSV$ . The existence of the initial stress is often unavoidable in the layered piezoelectric structures. The effect of initial stress on the reflection and transmission wave at the interface between two piezoelectric solids is therefore interesting. The effects of material gradient and initial stress on reflection coefficient of  $qP$  and  $qSV$  waves have been studied.

From the numerical results, the following conclusions can be drawn

1. For the incident plane wave the reflection coefficients of  $qP$  and  $qSV$  waves is evidently affected by the presence of the initial stresses. The effects of initial stresses on the reflection coefficient are dependent on the incident angle range.
2. Pre-stressed FGPM has the highest speed for reflected wave as compared to FGPM and piezoelectric medium. The speed of  $qP$  waves increases and that of  $qSV$  waves decreases in piezoelectric medium as the angle of incidence changes from normal to grazing.
3. Refection coefficient of  $qSV$  and  $qP$  waves is greater in FGPM and pre-stressed FGPM as compared to other media.

4. Material gradient of the medium makes the reflection coefficient of  $qP$  waves increasing and decreasing as the angle of incident changes from normal to grazing. It is noticed that the reflection coefficient of  $qP$  waves increase from  $0^0$  to around  $40^0$  and decreases onwards for the case of incident  $qP$  waves.
5. In the case of incident  $qP$  waves, reflection coefficient of  $qP$  waves decreases with the increase of initial stress  $\sigma_{xx}^0$  upto incident angle  $0^0 - 40^0$  and decreases afterward.
6. In the case of incident  $qP$  waves, reflection coefficient of  $qP$  waves increases with initial stress  $\sigma_{xz}^0$ . In the case of incident  $qSV$  waves reflection coefficient of  $qSV$  waves remain constant initially. Then it decreases with the increase of initial stress  $\sigma_{xz}^0$  upto incident angle  $150^0 - 40^0$  and decreases afterward.
7. In the case of incident  $qP$  waves, reflection coefficient of  $qP$  waves decreases with initial stress  $\sigma_{zz}^0$ . However, in the case of incident  $qSV$  waves the curves clearly show that the amplitude ratio of  $qSV$  first remains constant then decreases and again increases as the angle of incidence of  $qSV$  waves increases.

The present study can possibly be useful to geophysicist and metallurgists for analysis of rock and material structures through non-destructive testing. This study can also be useful in signal processing, sound system and wireless communication in addition to improvement of SAW wave devices and defense equipment.

## REFERENCES

- [1] Shana Z., Josse F., 1992, Reflection of bulk wave at a piezoelectric crystal-viscous conductive liquid interface, *Journal of the Acoustical Society of America* **91**: 854-860.
- [2] Noorbehesht B., Wade G., 1980, Reflection and transmission of plane elastic-wave at the boundary between piezoelectric materials and water, *Journal of the Acoustical Society of America* **67**: 1947-1953.
- [3] Chattopadhyay A., Saha S., 1996, Reflection and refraction of P wave at the interface of two monoclinic media, *International Journal of Engineering Science* **34** (11): 1271-1284.
- [4] Kaur J., Tomar S. K., 2004, Reflection and refraction of SH-wave at a corrugated interface between two monoclinic elastic half-spaces, *International Journal for Numerical and Analytical Methods in Geomechanics* **28**(15): 1543-1575.
- [5] Kyame J.J., 1949, Wave propagation in piezoelectric crystals, *Journal of the Acoustical Society of America* **21**: 159-167.
- [6] Yang J.S., 2006, A review of a few topics in piezoelectricity, *Applied Mechanics Reviews* **59**: 335-345.
- [7] Fang H., Yang J., Jiang Q., 2001, Surface acoustic wave propagating over a rotating piezoelectric half-space, *IEEE Transactions on Ultrasonics, Ferroelectrics and Frequency Control* **48**: 998-1004.
- [8] Wang Q., 2002, Wave propagation in a piezoelectric coupled solid medium, *Journal of Applied Mechanics* **69**: 819-824.
- [9] Yang J.S., Zhou H.G., 2005, An interface wave in piezoelectromagnetic materials, *International Journal of Applied Electromagnetics and Mechanics* **21**: 63-68.
- [10] Pang Y., Yue-Sheng W., 2008, Reflection and refraction of plane wave at the interface between piezoelectric and piezomagnetic media, *International Journal of Engineering Science* **46**: 1098-1110.
- [11] Sharma J.N., Walia V., Gupta S.K., 2008, Reflection of piezothermoelastic wave from the charge and stress free boundary of a transversely isotropic half space, *International Journal of Engineering Science* **46**: 131-146.
- [12] Chattopadhyay A., Saha S., Chakraborty M., 1997, Reflection and transmission of shear wave in monoclinic media, *International Journal for Numerical and Analytical Methods in Geomechanics* **21**(7): 495-504.
- [13] Sharma J.N., Walia V., 2007, Further investigations on rayleigh wave in piezothermoelastic materials, *Journal of Sound and Vibration* **301**: 189-206.
- [14] Abd-alla A.N., Alsheikh F.A., 2009, Reflection and refraction of plane quasilongitudinal wave at an interface of two piezoelectric media under initial stresses, *Archive of Applied Mechanics* **79**: 843-857.
- [15] Singh B., 2010, Wave propagation in a pre-stressed piezoelectric half-space, *Acta Mechanica* **211**: 337-344.
- [16] Guo X., Wei P., 2014, Effect of initial stress on the reflection and transmission wave at the interface between two piezoelectric half-spaces, *International Journal of Solids and Structures* **51**: 3735-3751.
- [17] Wang Z. K., Shang, F. L., 1997, Cylindrical buckling of piezoelectric laminated plates, *Acta Mechanica Solida Sinica* **18**: 101-108.
- [18] Weis R.S., Gaylord, T.K., 1985, Lithium niobate: summary of physical properties and crystal structure, *Applied Physics A* **37**: 191-203.